International Journal of Orthopaedics

Online Submissions: http: //www.ghrnet.org/index.php/ijo
doi: 10.17554/j.issn.2311-5106.2022.09.451

Int. J. of Orth. 2022 June 28; **9(3)**: 1682-1687
ISSN 2311-5106 (Print), ISSN 2313-1462 (Online)

ORIGINAL ARTICLE

Evaluation Methodology for Reoperation after Intramedullary Nailing for Femoral Shaft Fracture: A Quantitative Computer Tomography-based Finite Element Analysis

Hideyuki Mimata, PhD.1, Yusuke Matsuura, MD., PhD.2, Sei Yano, MD.2, Seiji Ohtori, MD., PhD.2, Mitsugu Todo, PhD.3

1 Interdisciplinary Graduate School of Engineering Sciences, Kyushu University, 6-1 Kasuga-Koen Kasuga-shi, Fukuoka 816-8580, Japan;
2 Department of Orthopeadic Surgery, Graduate School of Medicine, Chiba University, 1-8-1 Inohana, Chuo-ku, Chiba 260-8670, Japan;
3 Research Institute for Applied Mechanics, Kyushu University, 6-1 Kasuga-Koen Kasuga-shi, Fukuoka 816-8580, Japan.

Conflict-of-interest statement: The author(s) declare(s) that there is no conflict of interest regarding the publication of this paper.

Correspondence to: Hideyuki Mimata, Interdisciplinary Graduate School of Engineering Sciences, Kyushu University, 6-1 Kasuga-Koen Kasuga-shi, Fukuoka 816-8580, Japan.
Email: hideyuki.mimata@gmail.com
Telephone: +81-03-3785-3059
Fax: +81-03-3785-3066

Received: April 7, 2022
Revised: May 5, 2022
Accepted: May 10 2022
Published online: June 28, 2022

ABSTRACT

AIM: In a few cases of intramedullary nailing for femoral shaft fractures, nonunion due to insufficient fixation has been experienced. Although good results have been reported with the exchange nailing and the plate augmentation for reoperation, no method has been established to quantitatively evaluate postoperative instability, and it is not clear how the mechanical condition, including callus, is improved. In this study, Quantitative CT-based finite element analysis was used to quantify postoperative instability and to evaluate the mechanical effects of reoperation.

MATERIALS AND METHODS: A reoperation model (exchange nailing and plate augmentation) was created in addition to the actual surgery model using a CT of a patient who had an intramedullary nailing for a femoral shaft fracture. Finite element analysis was performed to evaluate the tensile failure risk of the callus at the fracture site, which is considered to contribute significantly to bone union.

RESULTS: In the actual surgery model with 11 mm diameter nails, 11.4% of callus showed tensile failure under axial loading of 3 times body weight, but this was reduced to 6.5% when the nail was changed to 13 mm diameter and 5.8% with the augmentation of a 5-hole plate.

CONCLUSION: The augmentation plate on the lateral side was mechanically shown to promote union similar to exchange nailing.

Key words: Femoral shaft fracture; Intramedullary nailing; Exchange nailing; Plate augmentation; Finite element analysis; Callus

Mimata H, Matsuura Y, Yano S, Ohtori S, Todo M. Evaluation Methodology for Reoperation after Intramedullary Nailing for Femoral Shaft Fracture: A Quantitative Computer Tomography-based Finite Element Analysis. *International Journal of Orthopaedics* 2022; **9(3)**: 1682-1687 Available from: URL: http: //www.ghrnet.org/index.php/ijo/article/view/3281

List of abbreviations
CT: Computer tomography
QCT/FEA: Quantitative CT-based finite element analysis
HA: Hydroxyapatite

INTRODUCTION

Good union rate has been obtained with intramedullary nailing for femoral shaft fractures, while nonunion have been reported

in 3.1%-12.5% of cases[1-5]. Factors associated with nonunion include open fractures, smoking, screw failure, and improper dynamization[4-7]. Especially hypertrophic nonunion is thought to be caused by instability of the fracture site[8,9]. Exchange nailing or plate augmentation is selected as the treatment for nonunion after intramedullary nailing for femoral shaft fracture. The diameter of an intramedullary nail contributes to overall bone stiffness after surgery, and a decreasing trend in nonunion rate has been reported with increasing intramedullary nail diameters, even though the difference is not clinically significant[10]. For a plate augmentation, a higher union rate has been reported compared to an exchange nailing[11]. However, there is no established mechanical procedure for evaluating postoperative instability or appropriate reoperation.

With regard to the mechanical evaluation of bone, since the material properties of bone were obtained from fresh-frozen cadavers by Keyak et al[12] and Keller[13] using mechanical tests, Quantitative CT-based finite element analysis (QCT/FEA) has been established, and good correlations have been reported in validation tests in various bones[14-17]. However, the empirical equations for material properties used in these models are derived from experiments on mature bone, and no finite element model has ever been developed applying inhomogeneous material properties based on CT values to callus. Suzuki et al. developed conversion equations between callus density and its Young's modulus and yield stress by experiments with New Zealand white rabbits[18], allowing the derivation of callus material properties based on CT values. They have also validated the QCT/FEA during the maturation process using these equations.

We used QCT/FEA during bone healing process to evaluate the postoperative instability of intramedullary nailing for femoral shaft fracture and to compare reoperation approaches for nonunion. There are reports that compression is better than tension at the fracture site for bone healing, or that appropriate compression is good for bone healing, based on experiments with sheep[19,20]. Therefore, with the hypothesis that tensile forces inhibit bone healing, we focused on the tensile failure risk of the callus. The aim of this study was to establish a quantitative assessment of instability after intramedullary nailing for femoral shaft fracture and after reoperation with exchange nailing or plate augmentation for nonunion using QCT/FEA.

MATERIAL & METHOD

Subject

The subject (51-year-old, male) was injured in a fall when he collided with an oncoming car while riding a motorcycle. He was transported by ambulance and a left femoral shaft fracture was found. On the same day, emergency operation was performed using an intramedullary nail (T2® femoral nail φ11 mm x L360 mm, Stryker Corp., Kalamazoo, Michigan, USA). For postoperative rehabilitation, half body weight was loaded until 4 weeks postoperatively, then full body weight was loaded thereafter. However, at 6 months postoperatively, a hypertrophic nonunion was suspected (Figure 1). CT imaging was performed with a CT system (Aquilion ONE, Canon Medical Systems Inc., Tochigi, Japan), and CT data with a slice thickness of 0.5 mm and a pixel size of 0.45 mm was used. For calibration of hydroxyapatite(HA)-equivalent density, CT scan was taken with a bone density calibration phantom (B-MAS200, Kyoto Scientific, Kyoto, Japan).

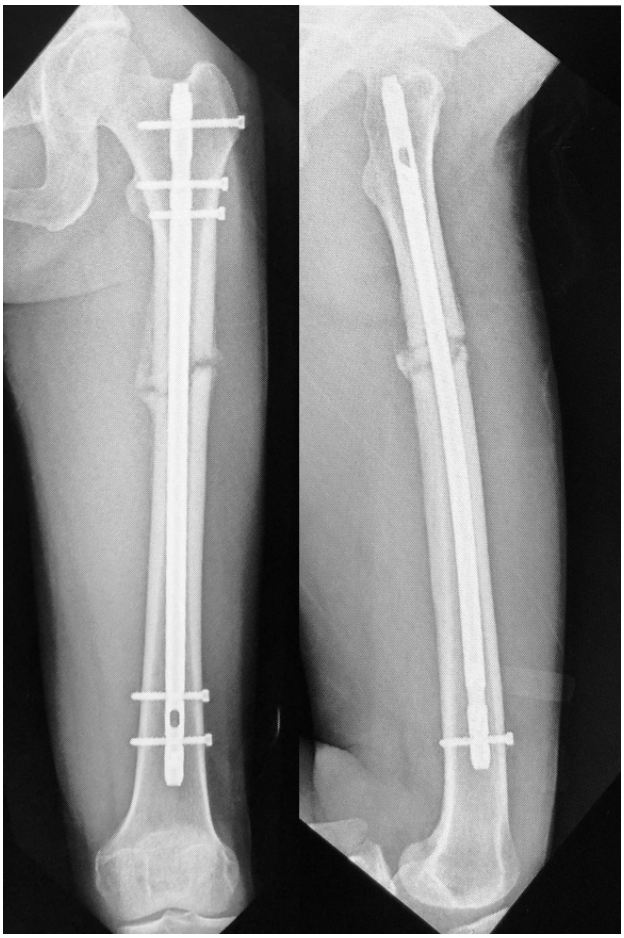

Figure 1 Radiograph 6 months after surgery. Hypertrophic nonunion is suspected because callus is formed but lacks continuity.

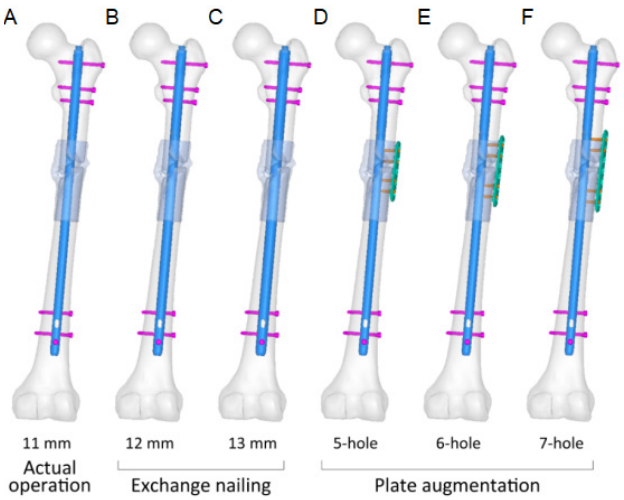

Figure 2 Finite element models. Actual surgery model with 11 mm diameter nail, exchange nailing models (12 mm, 13 mm), and plate augmentation models (5-hole, 6-hole, 7-hole) were constructed.

Finite element modeling

QCT/FEA software (MECHANICAL FINDER version 11.0 Extended Edition, Research Center of Computational Mechanics, Inc., Tokyo, Japan) was utilized for the static and elastic analysis with contact nonlinearity. Geometries of intramedullary nails, plates(LCP Plates 3.5, Synthes, Raynham, MA, USA), and screws were created using 3D modeling software (Metasequoia 4.7, Tetraface Inc., Tokyo, Japan). The model consists of proximal and distal femoral fragments, a callus, an intramedullary nail, a plate, and screws. In addition to the actual intramedullary nailing model with 11mm diameter nail (A), the following five models were constructed: exchange nailing with 12 mm (B) and 13 mm (C) diameter nail, plate augmentation with

5-hole (D), 6-hole (E), and 7-hole (F) plate (Figure 2). The bi-cortical locking screws for plate fixation are inserted laterally and passes behind the nail. The plate is fixed to the proximal and distal bone fragments with two screws each and the longer (more holes) the plate, the wider the proximal-distal screw distance. To reduce the effect of artifacts, the corresponding region was modeled independently, and an upper density limit was set (Figure 3A). The mesh is constructed with first-order tetrahedral elements with a minimum size of 0.375 mm and a general size of 3.0 mm, and the number of elements in each model is approximately 3-4 million. Mesh convergence was evaluated in terms of total strain energy. The ratio of the minimum and general size was kept constant, and the error was confirmed to be within approximately 1% relative to the finest model with the general size of 1.5 mm.

Material Properties

HA equivalent density, ρ_{HA} of bone and callus was obtained from CT value by calibration using phantom. Next, Young's modulus and yield stress of the bone and callus were assigned to each element according to the equations of Matsuyama et al[21] and Suzuki et al[18], respectively (Table 1). The critical stress was set to 0.8 times the yield stress for both bone and callus according to the protocol of Bessho et al[14]. Intramedullary nails, plates, and screws had material properties of Ti6Al4V. The upper density limit was set at 600 mg/cm^3 for cancellous bone artifact region and 1500 mg/cm^3 for cortical one, based on the density distribution of the healthy side. Contact conditions were defined on the interfaces of the intramedullary nail to the bone/callus, the intramedullary nail to the screws, and the plate to the bone/callus, and the coefficient of friction on the contact surfaces was set to 0.0.

Boundary Condition

A load of three times the body weight (1911 N) was applied to the bone head, since the mechanical axial component of the maximum load during gait is approximately three times the body weight in the report by Heller et al[22] (Figure 3B). The direction of load was always oriented from the center of the femoral head to the center of the knee joint. The distal end of the femur was fully constrained.

Evaluation Method

We focused on the tensile failure risk of the callus between bone fragments, which may contribute to strength, since Claes et al. reported that the force acting on fracture site during the bone healing process is better in compression than in tension in their experiments with sheep[19]. The tensile failure risk of each element is determined using the critical stress as follows.

$$\text{Tensile Failure Risk} = \frac{\text{Maximum principal stress}}{\text{Critical stress}}$$

Then, the volume ratio of the elements with a tensile failure risk greater than one in the callus region between the bone fragments was employed as an index, as shown in Figure 4.

$$\text{Tensile Failure Ratio} = \frac{\text{Element volume with tensile failure risk} \geq 1}{\text{Volume of callus between bone fragments}}$$

In addition, relative displacements of the proximal and distal bone fragments were evaluated at the medial and lateral sides near the fracture site to assess fragment instability.

RESULTS

Figure 5 shows the elements of callus with a tensile failure risk of 50% or greater at 6 months after surgery. Focusing on the region between the bone fragments, many elements show a higher tensile

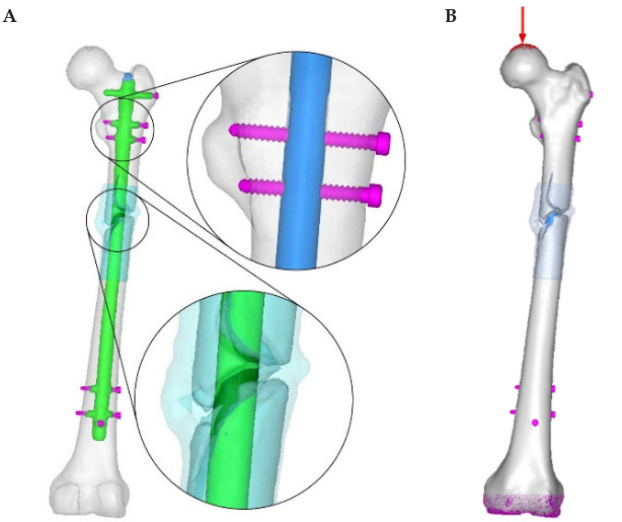

Figure 3 (A) Detail of finite element model. Screws have clearance between screw holes as in the real ones. Artifact regions are modeled separately to set the upper density limit. (B) Boundary condition. Three times the body weight is applied on the femoral head in the direction of the mechanical axis.

Table 1 Material properties, where ρ_{HA} means hydroxyapatite equivalent density (g/cm^3). Yield stress and critical stress are not used in the analysis because of the material linear analysis, but critical stress is used when evaluating the tensile failure risk.

	Young's modules (MPa)	Yield stress (MPa)	Critical Stress (MPa)	Poisson's ratio
Bone	$1530.6\ \rho_{HA}^{1.9213}$	$116.64\ \rho_{HA}^{1.8952}$	Yield stress*0.8	0.3
Callus	$0.2391e^{8.00\rho_{HA}}$	$30.49\ \rho_{HA}^{2.41}$	Yield stress*0.8	0.3
Nail (Ti6Al4V)	113000	909	999	0.315
Screw (Ti6Al4V)				
Plate (Ti6Al4V)				

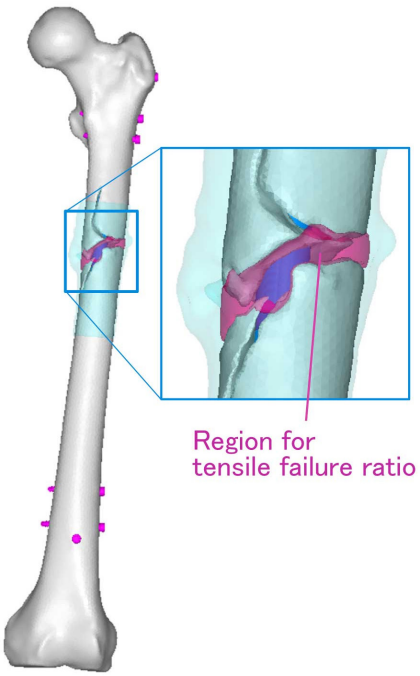

Figure 4 Callus region used to derive tensile failure ratio. The region between bone fragments considered to contribute to bone strength was used.

failure risk on lateral side. In the load dependence of the tensile failure ratio, 11.4% of the regions had tensile failure at three times the body weight (Figure 6). Tensile failure risk in each reoperated model was reduced in the lateral side, especially in exchange nailing model with 13 mm diameter nail and all plate augmentation models (Figure 7). The actual surgery model showed a tensile failure ratio of 11.4%, while exchange nailing with12 and 13 mm diameter nail decreased it to 9.7% and 6.5% , respectively (Figure 8). The plate augmentation was more effective with closer screw distance between bone fragments, with tensile failure ratio of 5.8%, 6.5%, and 6.6% in 5, 6, and 7-hole model, respectively.

The distance between bone fragments was 0.8 mm closed on the medial side and 0.2 mm opened on the lateral side when three times body weight was applied in the actual surgery model (Figure 9). Overall movement was suppressed when the nail was exchanged to a larger diameter nail. Especially in the 13 mm diameter model, the distance was reduced even on the lateral side (medial: -0.5 mm, lateral: -0.1 mm). Plate augmentation suppressed the lateral opening, which was -0.7 mm on the medial side and -0.1 mm on the lateral side in the 5-hole plate model.

DISCUSSION

The tensile failure ratio was about 11% in the actual surgery model (11 mm diameter) at three times body weight loading, indicating the possibility of future nonunion. A cut-off value for nonunion is expected to be derived by increasing the number of cases in the future. However, even without a cut-off value, it could be useful for relative evaluation as an index that reflects actual material properties of callus.

In this study, the loading condition was applied to the femoral head in the direction of the mechanical axis, resulting in a tensile force on the lateral side. Consequently, the distance between the fragments was closed on the medial side and opened on the lateral side in the actual surgery model. Exchanging the nail with larger diameter ones increased overall stiffness and reduced the bending, leading to a decrease in medial compression and lateral tension. Movement on the lateral side also shifted from tensile to compressive when exchanging to the 13 mm diameter nail, and this contributed to the significant reduction in the tensile failure ratio. Claes et al. reported that compression at the fracture site is superior to tension and shear

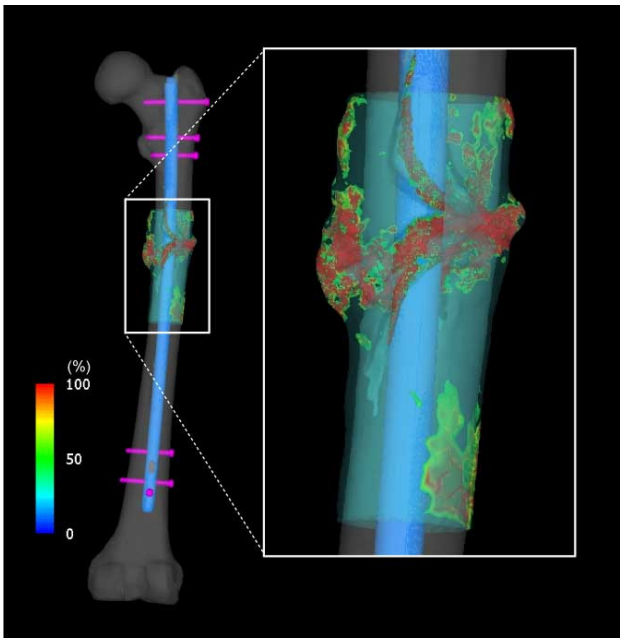

Figure 5 Elements with greater than 50% tensile failure risk at three times body weight for actual surgery model. Callus with a high tensile failure risk at the fracture site are concentrated on the lateral side.

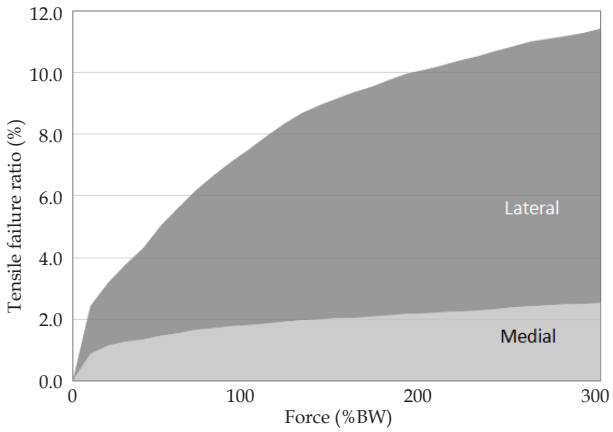

Figure 6 Load change in tensile failure ratio of the actual surgery model.

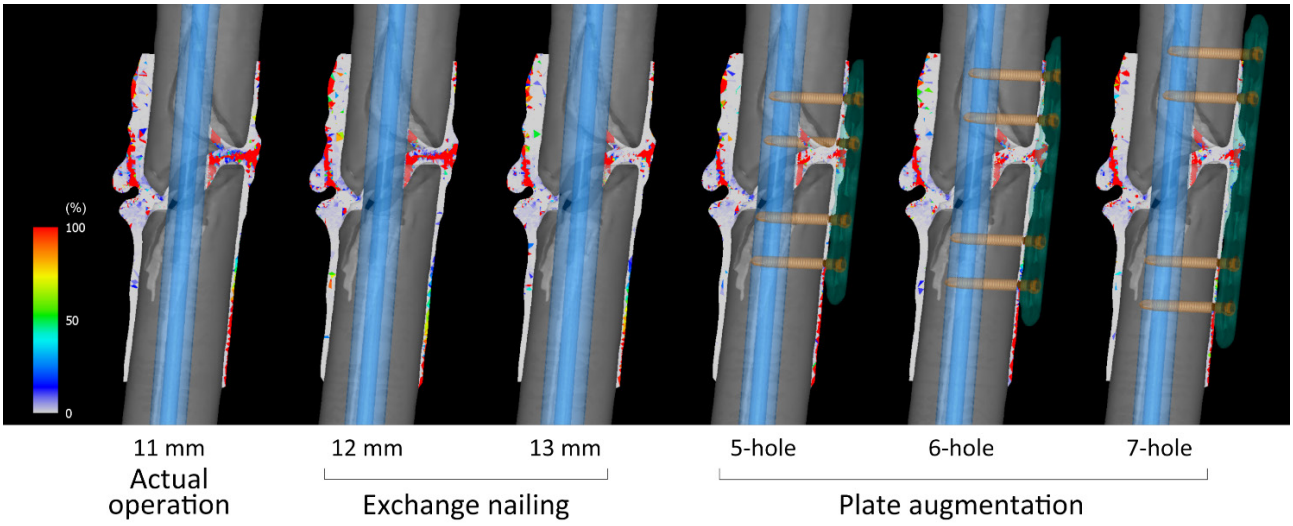

Figure 7 Cross-sectional view of the tensile failure risk of the callus. In particular, the exchange nailing with 13 mm diameter nail and the plate augmentation models reduce the tensile failure risk on the lateral side at the fracture site.

for revascularization and bone healing in their experiments with sheep[19]. Experiments by Epari et al. have also shown that fixation with appropriate compressive stiffness of the fracture site is better for bone healing[20]. These factors support that raising the diameter up to 13 mm in this case would have a positive effect on bone fusion. Serrano et al. also reported that the nonunion rate tended to decrease as the diameter of the intramedullary nail increased, even though the difference was not significant[10]. The difference between 11 mm and 12 mm is smaller than that between 12 mm and 13 mm, which may be due to the fact that the second moment of area acts in proportion to the fourth power of the diameter and that the 11 mm diameter of the T2® femoral nail has an 11.5 mm diameter in the proximal part.

Plate augmentation directly fixates the lateral side and works toward closing the bone fragments, so-called "tension band effect", thus reducing the tensile failure of the callus. The smaller screw distance between the bone fragments (shorter plates between them) results in less relative displacement between the fragments, and therefore also less tensile failure ratio. The best plate augmentation with 5-hole plate showed comparable tensile failure ratio to exchange nailing with 13 mm diameter nail, consistent with the report by Medlock et al. that plate augmentation is as good as or better than exchange nailing as a reoperation for nonunion[11]. Not only in terms of surgical difficulty, but also from a mechanical aspect, the plate augmentation could be an option for reoperation. It was also suggested that screw fixation closer to the fracture site on both bone fragments would be more effective for plate augmentation.

Tensile failure ratio of callus with CT-based material properties can be used to evaluate mechanical status on a subject-specific and chronological change and is shown to be useful in determining preoperative surgical methods. In this study, the exchange nailing was just a change in nail diameter and the plate augmentation was just a change in plate length, but many variations are possible, such as nail length, with/without anteroposterior screw, and number of screws for exchange nailing, and position, single/bi-cortical screw and number of screws for plate augmentation. In the future, surgical procedures are expected to be determined not only by surgical difficulty and infection risk, but also by mechanical evaluation.

This study has the following limitations. The first is that this is an analysis of a single case, and the cut-off value for the tensile failure ratio leading to nonunion is not clear. In the future, the cutoff value can be derived by following the number of cases and time-series changes. Second, the loading condition is a simple axial load. If a load during walking, in which muscle force is also applied, is used, the results may change slightly due to the addition of rotation and other factors. Third, this study uses postoperative CT data, which is affected by artifacts. However, the effect is considered small because an upper limit is set for Young's modulus and the intramedullary nail is sufficiently hard. Fourth, it is a material linear analysis. This is because material nonlinear analysis in addition to contact analysis is very time consuming. It is important to verify whether the same index can be used for material nonlinear analysis. Fifth, the biological effects of the reoperation were not considered. The effects of reaming and chipping performed during exchange nailing cannot be evaluated and are limited in their accurate expression in these finite element models.

CONCLUSION

Mechanical assessment can be incorporated into the decision process for reoperation by constructing a CT-based inhomogeneous model and assessing the tensile failure risk of the callus at the fracture site with finite element analysis. The plate augmentation was mechanically equivalent in fixation to exchange nailing and can be an option in reoperation for nonunion.

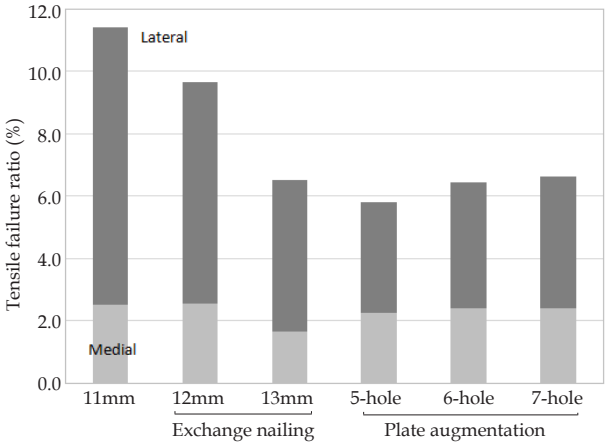

Figure 8 Tensile failure ratio of each model. Reduction was seen with smaller screw distance for plate augmentation and was comparable to exchange nailing with 13mm diameter nail.

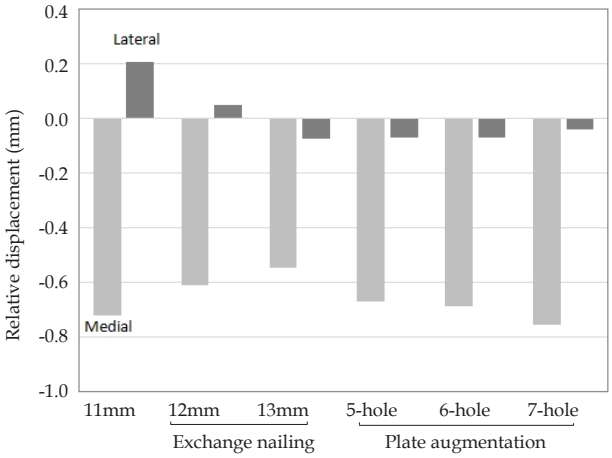

Figure 9 Gap changes between bone fragments. Lateral opening changes to close after exchange nailing with 13 mm diameter nail and plate augmentations.

REFERENCE

1. Koso RE, Terhoeve C, Steen RG, Zura R. Healing, nonunion, and re-operation after internal fixation of diaphyseal and distal femoral fractures: a systematic review and meta-analysis. *Int Orthop*. 2018; **42(11)**: 2675-83. Epub 2018/03/08. [DOI: 10.1007/s00264-018-3864-4]; [PMID: 29516238].
2. Metsemakers WJ, Roels N, Belmans A, Reynders P, Nijs S. Risk factors for nonunion after intramedullary nailing of femoral shaft fractures: Remaining controversies. *Injury*. 2015; **46(8)**: 1601-7. Epub 2015/05/12. [DOI: 10.1016/j.injury.2015.05.007]; [PMID: 26026201].
3. Pihlajamäki HK, Salminen ST, Böstman OM. The treatment of nonunions following intramedullary nailing of femoral shaft fractures. *J Orthop Trauma*. 2002; **16(6)**: 394-402. [DOI: 10.1097/00005131-200207000-00005]; [PMID: 12142827].
4. Taitsman LA, Lynch JR, Agel J, Barei DP, Nork SE. Risk factors for femoral nonunion after femoral shaft fracture. *J Trauma*. 2009; **67(6)**: 1389-92. [DOI: 10.1097/TA.0b013e318182afd0]; [PMID: 19704386].
5. Society COT. Nonunion following intramedullary nailing of the femur with and without reaming. Results of a multicenter randomized clinical trial. *J Bone Joint Surg Am*. 2003; **85(11)**:

2093-6]; [PMID: 14630836].
6. Watanabe Y, Takenaka N, Kobayashi M, Matsushita T. Infra-isthmal fracture is a risk factor for nonunion after femoral nailing: a case-control study. *J Orthop Sci.* 2013; **18(1)**: 76-80. Epub 2012/10/11. [DOI: 10.1007/s00776-012-0316-7]; [PMID: 23053587].
7. Claes L, Eckert-Hübner K, Augat P. The fracture gap size influences the local vascularization and tissue differentiation in callus healing. *Langenbecks Arch Surg.* 2003; **388(5)**: 316-22. Epub 20030909. [DOI: 10.1007/s00423-003-0396-0]; [PMID: 13680236].
8. Ortega GR, Cunningham BP. Femoral Shaft Nonunions. In: Agarwal A, editor. Nonunions: Diagnosis, Evaluation and Management. Boston, MA: Springer US; 2018. p. 227-42.
9. Megas P, Panagiotis M. Classification of non-union. *Injury*. 2005; **36 Suppl 4**: S30-7. [DOI: 10.1016/j.injury.2005.10.008]; [PMID: 16291321].
10. Serrano R, Mir HR, Gorman RA, Karsch J, Kim R, Shah A, Maxson B, Infante A, Watson D, Downes K, Sanders RW. Effect of Nail Size, Insertion, and Δ Canal-Nail on the Development of a Nonunion After Intramedullary Nailing of Femoral Shaft Fractures. *J Orthop Trauma*. 2019; **33(11)**: 559-63. [DOI: 10.1097/BOT.0000000000001585]; [PMID: 31464856].
11. Medlock G, Stevenson IM, Johnstone AJ. Uniting the un-united: should established non-unions of femoral shaft fractures initially treated with IM nails be treated by plate augmentation instead of exchange IM nailing? A systematic review. *Strategies Trauma Limb Reconstr.* 2018; **13(3)**: 119-28. Epub 20181113. [DOI: 10.1007/s11751-018-0323-0]; [PMID: 30426320]; [PMCID: PMC6249146].
12. Keyak JH, Lee IY, Skinner HB. Correlations between orthogonal mechanical properties and density of trabecular bone: use of different densitometric measures. *J Biomed Mater Res.* 1994; **28(11)**: 1329-36. [DOI: 10.1002/jbm.820281111]; [PMID: 7829563].
13. Keller TS. Predicting the compressive mechanical behavior of bone. *J Biomech.* 1994; **27(9)**: 1159-68. [DOI: 10.1016/0021-9290(94)90056-6]; [PMID: 7929465].
14. Bessho M, Ohnishi I, Matsuyama J, Matsumoto T, Imai K, Nakamura K. Prediction of strength and strain of the proximal femur by a CT-based finite element method. *J Biomech.* 2007; **40(8)**: 1745-53. Epub 2006/10/10. [DOI: 10.1016/j.jbiomech.2006.08.003]; [PMID: 17034798].
15. Imai K, Ohnishi I, Bessho M, Nakamura K. Nonlinear finite element model predicts vertebral bone strength and fracture site. *Spine* (Phila Pa 1976). 2006; **31(16)**: 1789-94. [DOI: 10.1097/01.brs.0000225993.57349.df]; [PMID: 16845352].
16. Matsuura Y, Kuniyoshi K, Suzuki T, Ogawa Y, Sukegawa K, Rokkaku T, Thoreson AR. An KN. Takahashi K. Accuracy of specimen-specific nonlinear finite element analysis for evaluation of radial diaphysis strength in cadaver material. *Comput Methods Biomech Biomed Engin.* 2015; **18(16)**: 1811-7. Epub 2014/11/06. [DOI: 10.1080/10255842.2014.974579]; [PMID: 25374112].
17. Dragomir-Daescu D, Op Den Buijs J, McEligot S, Dai Y, Entwistle RC, Salas C, Melton LJ, Bennet KE, Khosla S, Amin S. Robust QCT/FEA models of proximal femur stiffness and fracture load during a sideways fall on the hip. *Ann Biomed Eng*. 2011; **39(2)**: 742-55. Epub 2010/10/29. [DOI: 10.1007/s10439-010-0196-y]; [PMID: 21052839]; [PMCID: PMC3870095].
18. Suzuki T, Matsuura Y, Yamazaki T, Akasaka T, Ozone E, Matsuyama Y, Mukai M, Ohara T, Wakita H, Taniguchi S, Ohtori S. Biomechanics of callus in the bone healing process, determined by specimen-specific finite element analysis. *Bone*. 2020; **132**: 115212. Epub 2019/12/28. [DOI: 10.1016/j.bone.2019.115212]; [PMID: 31891786].
19. Claes L, Meyers N, Schülke J, Reitmaier S, Klose S, Ignatius A. The mode of interfragmentary movement affects bone formation and revascularization after callus distraction. *PLoS One.* 2018; **13(8)**: e0202702. Epub 2018/08/23. [DOI: 10.1371/journal.pone.0202702]; [PMID: 30138362]; [PMCID: PMC6107229.t]
20. Epari DR, Kassi JP, Schell H, Duda GN. Timely fracture-healing requires optimization of axial fixation stability. *J Bone Joint Surg Am.* 2007; **89(7)**: 1575-85. [DOI: 10.2106/JBJS.F.00247]; [PMID: 17606797].
21. Matsuyama Y, Matsuura Y, Suzuki T, Akasaka T, Himeno D, Yamazaki A, Ozone E, Mukai M, Yamazaki T, Ohara T, Taniguchi S, Wakita H, Kuniyoshi K, Ohtori S, Sasho T. New material property conversion equation for bone strength measurement for CT-based finite element modeling. *Chiba medical journal.* 2020; **96(2)**: 41-6. [DOI: 10.20776/S03035476-96E-2-P41].
22. Heller MO, Bergmann G, Kassi JP, Claes L, Haas NP, Duda GN. Determination of muscle loading at the hip joint for use in pre-clinical testing. *J Biomech.* 2005; **38(5)**: 1155-63. [DOI: 10.1016/j.jbiomech.2004.05.022]; [PMID: 15797596].